Available online at www.sciencedirect.com
SCIENCE DIRECT®
Journal of Sound and Vibration 283 (2005) 47–67
JOURNAL OF SOUND AND VIBRATION
www.elsevier.com/locate/jsvi

The equivalent impedance of power-minimising vibration controllers on plates

L. Benassi*, S.J. Elliott

Institute of Sound and Vibration Research, University of Southampton, Southampton SO17 1BJ, UK

Received 25 September 2003; accepted 30 March 2004

Abstract

Strategies for the suppression of plate vibration are investigated by considering the equivalent impedance of power-minimising vibration controllers. The total power transmitted to a plate by both a primary and secondary point forces is used as a function to be minimised. If the system is linear, then the total power has a known minimum value that is associated with an optimal solution for the secondary force. This minimum power, applied to infinite and finite plates, has been compared to the power reduction that can be achieved with passive vibration treatments. The ratio of the optimal secondary force and the resultant velocity at the secondary force location is termed the equivalent impedance of the active control system, and if only a single primary source is present, this equivalent impedance is entirely reactive but generally unrealisable.

The approximation of the equivalent impedance by lumped parameter systems is considered. In particular, passive controllers, based on springs and dampers, have been analysed, although, in many practical applications, a rigid ground is not available to react these components off. The importance of this work lies in the practical approximation of these equivalent impedances with realisable passive systems.

1. Introduction

Vibration control of flexible structures is an important issue in many engineering applications, especially for the precise operation performances in aerospace systems, satellites, flexible

*Corresponding author.18a Derby Street, Cambridge CB3 9JE, UK. Tel.: +44-23-8059-2689; fax: +44-23-8059-3190.

E-mail address: lb@isvr.soton.ac.uk (L. Benassi).

0022-460X/$ - see front matter © 2004 Elsevier Ltd. All rights reserved.
doi:10.1016/j.jsv.2004.03.060

manipulators, etc. Balancing the stringent performance objectives of modern structures such as superior strength and minimal weight introduces a dynamic component that needs to be considered. Depending on the application, low structural damping can lead to problems such as measurement inaccuracy of attached equipment, transmission of acoustic noise or structural failure. Two types of control methods are generally used to solve this problem: passive control and active control. Passive vibration control and the use of tuned systems can be effective on single frequency vibrations [1]. This work considers the possibility of broadband control of a distributed system such as a panel using local vibration controllers.

A description has been given in Bardou et al. [2] and Brennan et al. [3,4] of the performance of two possible strategies that can be used to design an active vibration controller: total power minimisation and maximisation of the power absorption of the secondary source.

In this paper, the total power generated by all the forces acting on the structure is used as a function to be minimised [5]. This approach has also been used as a noise control technique [6,7]. If we assume the system to be linear such that the velocity fields produced by the forces can be superimposed, then the total power has a known minimum value that is associated with an optimal solution [6–9]. This solution can be compared to what the passive treatments manage to accomplish. Since this solution is optimal, no other strategy can perform better. The question is then how well a certain passive control scheme performs with respect to the optimal solution when the optimal impedance is replaced with its equivalent passive approximation, as shown in Fig. 1. This is one of the main issues discussed here. The passive impedance, Z, in Fig. 1(b) is assumed to reach off an inertial ground, in order to be consistent with the single secondary force in Fig. 1(a). In practice it may be possible for this force to be reached off a proof-mass, in an inertial actuator arrangement. The additional complexities that this generates for the control system and its performance are addressed in a companion paper [10].

A lot of work has been carried out in order to synthesise load impedances which achieve desired performances (using semi-definite programming, for example, by Titterton [11]), and in this study optimal impedances and impedances generated by passive devices (also studied by Guicking et al.

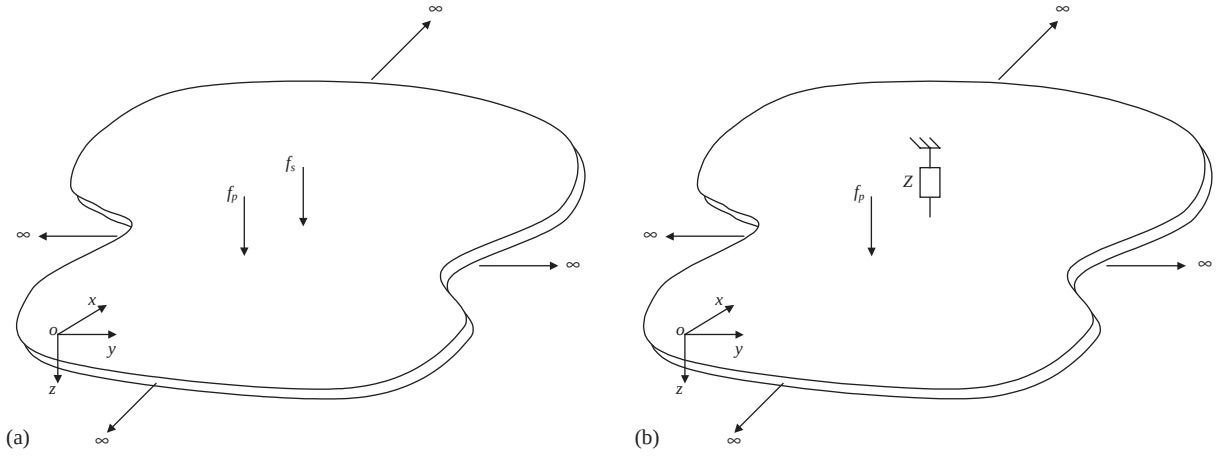

Fig. 1. (a) A point primary force and a point secondary force applied to an infinite thin plate. (b) A point primary force and an equivalent impedance applied to an infinite thin plate.

[12]) will be compared. The goal is to use these devices in order to reduce the total power, acting on a local basis [13]. Also, unlike most of the literature on this subject, the primary disturbance will be considered to be broadband rather than single frequency [11,14], and so the realisability of the equivalent impedance must be addressed.

One of the limitations of some of the models presented in the literature is that the primary force and the secondary control force are acting along the same axis. In real systems, there will inevitably by some mismatch between the point of application of the primary force and the point of application of the secondary force. This issue has been addressed by Jenkins et al. [15], and their results for an infinite plate show that appreciable reductions in total power can only be achieved if the secondary force is applied at a distance within $3\lambda_f/8$ from the primary force, where λ_f is the flexural wavelength in the receiving structure at the frequency of interest.

Infinite plates will be considered first in Section 2 and finite plates will then be analysed in Section 3. In particular a flexible plate, clamped on two edges and free on the other two, will be considered. In Section 4, the optimisation of the spring/damper approximation to the equivalent impedance is discussed, followed by the conclusions in Section 5.

2. Equivalent impedance for global control of vibrating infinite plates

In order to analyse the problems described in the introduction, we now examine a single point secondary force f_s separated by a distance r from a point primary force, f_p, both forces being applied along the z-axis on an infinite plate. This configuration is depicted in Fig. 1(a). The expression for the driving point mobility $Y_{00} = \dot{z}_0(\omega)/f_0(\omega)$ for an infinite plate, where $\dot{z}_0(\omega)$ is the velocity in the z direction, evaluated at a point $P_0 = (x_0, y_0)$, and $f_0(\omega)$ is the excitation force at P_0, is given by

$$Y_{00} = \frac{\omega}{8Dk^2} = \frac{1}{8\sqrt{Dm}}, \tag{1}$$

where $D = EI/(1-\upsilon^2)$ is the plate's bending stiffness, E is its Young's modulus, $I = h^3/12$, where h is the plate thickness, υ is Poisson's ratio, $m = \rho h$ is the mass per unit area, and ρ is the density of the plate material. It is important to note that Y_{00} is independent of frequency and it is real. The transfer mobility, between two points $P_1 = (x_1, y_1)$ and $P_0 = (x_0, y_0)$, $Y_{10} = \dot{z}_1(\omega)/f_0(\omega)$ is given by [16]

$$Y_{10} = \frac{\omega}{8Dk^2}\left[H_0^{(2)}(kr) - H_0^{(2)}(-\mathrm{j}kr)\right], \tag{2}$$

where $r = \sqrt{(x_1-x_0)^2 + (y_1-y_0)^2}$ is the distance between the points, $k = \omega/c_D$, $c_D = (D/m)^{1/4}\sqrt{\omega}$ is the phase velocity, and $H_0^{(2)}(\cdot)$ is the second kind of Hankel function of 0th order. This function can be written as

$$H_0^{(2)}(kr) = J_0(kr) - \mathrm{j}\,Y_0(kr), \tag{3}$$

where $J_0(kr)$ is the 0th order Bessel function of the first kind and $Y_0(\cdot)$ is the 0th order Bessel function of the second kind. While $H_0^{(2)}(kr)$ has got real and imaginary parts, $H_0^{(2)}(-\mathrm{j}kr)$ is entirely imaginary.

It is now possible to define a cost function that will be used as the reference for all the remaining computations. The chosen cost function is the total power supplied to the plate, which is given by the sum of the power Π_p due to the primary force acting in P_0 and the power Π_s due to the secondary force acting in P_1. It can be expressed as

$$\Pi = \Pi_p + \Pi_s \tag{4}$$

and rewritten considering that the total power is also one-half of the real part of the forces times the complex transverse velocity of the plate at the position of the application of the forces. This total power can also be written as [15]

$$\Pi = \tfrac{1}{2}\mathrm{Re}\left\{f_p^* v_p + f_s^* v_s\right\} = A\left|f_s\right|^2 + f_s^* b + b^* f_s + c, \tag{5}$$

which is a quadratic form where the parameters of the last term of Eq. (5) are

$$A = \tfrac{1}{2}\mathrm{Re}(Y_{11}), \qquad b = \tfrac{1}{2}\mathrm{Re}(Y_{10}) f_p, \qquad c = \tfrac{1}{2}|f_p|^2 \mathrm{Re}(Y_{00}) \tag{6-8}$$

where Y_{11} is the driving point mobility at location $P_1 = (x_1, y_1)$. In particular, the power of the primary force only, which provides the power of the system without any sort of treatment, is given by setting the secondary force in Eq. (5) to zero. This leads to

$$\Pi_p = c. \tag{9}$$

Eq. (5) has a well-defined minimum value

$$\Pi_{\mathrm{opt}} = c - \frac{|b|^2}{A}, \tag{10}$$

which is associated with an optimal secondary force f_{so} given by [9]

$$f_{\mathrm{so}} = -\frac{b}{A} = -\frac{\mathrm{Re}(Y_{10})}{\mathrm{Re}(Y_{11})} f_p. \tag{11}$$

In the particular case of an infinite plate, from Eq. (1) follows that

$$\mathrm{Re}(Y_{00}) = Y_{00}, \tag{12}$$

and from Eqs. (2) and (3) the real part of the transfer mobility for an infinite plate is given by

$$\mathrm{Re}(Y_{10}) = Y_{00} J_0(kr). \tag{13}$$

Thus the optimal solution in Eq. (11) can be rewritten as [14]

$$f_{\mathrm{so}} = -J_0(kr) f_p \tag{14}$$

and its corresponding power is given by

$$\Pi_{\mathrm{opt}} = [1 - J_0^2(kr)]\Pi_p. \tag{15}$$

The effectiveness of the optimal solution can be established by comparing Eq. (15) with the power input due to the primary disturbance f_p, given by Eq. (9). Eq. (15) is plotted in Fig. 2 as a function of kr. The optimal secondary force significantly reduces the total power supplied to the plate for values of kr below about 1. However, this attenuation tends to zero for larger values of kr. Thus placing the secondary force close to the primary force allows the system to perform well over a broad range of frequencies.

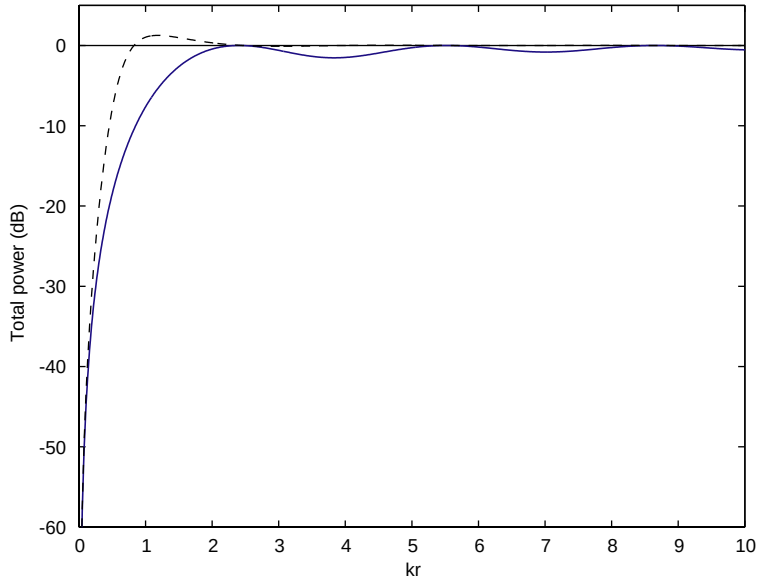

Fig. 2. Total power transmitted to an infinite plate, normalized to that due to the primary force only (solid black), when the primary and optimal secondary forces are applied (faint blue), and when the secondary force is replaced by a spring, whose stiffness is given by Eq. (23) (dashed).

The optimal "equivalent" impedance that is presented to the system in order to obtain such attenuation in the total power is now computed. The velocity v_s of the base at P_1, where the secondary force is acting, is given by a combination of the effects of the primary force, f_p, and the secondary force, f_s, at P_1

$$v_s = Y_{10} f_p + Y_{11} f_s, \tag{16}$$

where $Y_{00} = Y_{11}$ in this case. If the secondary force f_s is chosen to be the optimal solution f_{so} described in Eq. (14) and substituting Eq. (14) into Eq. (16), the velocity of the base at P_1 as a function of the primary force, when the optimal solution is implemented, is found to be

$$v_{so} = [Y_{10} - Y_{11} J_0(kr)] f_p. \tag{17}$$

From Eq. (14) it follows that

$$f_p = -\frac{1}{J_0(kr)} f_{so}, \tag{18}$$

which substituted into Eq. (17) provides the equation for the equivalent impedance. This is given by

$$\begin{aligned} Z_{opt} &= \frac{f_{so}}{v_{so}} = -\frac{J_0(kr)}{Y_{10} - Y_{11} J_0(kr)} \\ &= -\frac{J_0(kr)}{Y_{11}[H_0^{(2)}(kr) - H_0^{(2)}(-\mathrm{j}kr) - J_0(kr)]}, \end{aligned} \tag{19}$$

and it expresses the impedance that the secondary optimal force is presenting to the system in order to minimise the cost function given by the total power. The numerator of Eq. (19) is real, and its denominator is purely imaginary, thus Z_{opt} is entirely reactive [6]. Considering only the first terms of the series expansion [17] of Eq. (19) in terms of kr, an approximated expression can be obtained

$$\frac{f_{\mathrm{so}}}{v_{\mathrm{so}}} \cong \frac{(kr)^2/4 - 1}{\mathrm{j}Y_{11}\left((kr)^2/\pi\right)\left(\gamma - 1 + \ln\, kr/2\right)}, \tag{20}$$

where $\gamma = 0.577$ is the Euler's constant. The primary drawback of this result is that the compensator is non-causal [18]. Eq. (20) can be further expanded into

$$\frac{f_{\mathrm{so}}}{v_{\mathrm{so}}} \cong \frac{1}{\mathrm{j}\omega}\frac{2\pi\sqrt{Dm}\left(\omega r^2 - 4\sqrt{D/m}\right)}{r^2\left(\gamma - 1 + \ln\, kr/2\right)} = \frac{k_a}{\mathrm{j}\omega}, \tag{21}$$

where the dependence on $1/\mathrm{j}\omega$ has been made explicit in order to be able to express the remaining term as a stiffness coefficient k_a. The low-frequency approximation of the stiffness coefficient k_a in Eq. (21) is given by

$$k_a \cong \frac{8\pi D}{r^2\left(1 - \ln kr/2 - \gamma\right)}. \tag{22}$$

For very low frequencies and separation distances $kr \cong 0.01$ in which case $\ln kr/2 \cong -5$, and therefore Eq. (22) can be rewritten as

$$k_a \cong \frac{8\pi D}{r^2(6 - \gamma)}. \tag{23}$$

The full expression for the equivalent impedance, Eq. (19), is plotted in Fig. 3, along with its passive approximation, given by a stiffness term $k_a/\mathrm{j}\omega$, where $k_a = 1.2 \times 10^6$ N/m, as computed from Eq. (23) for the 1.85 mm plate when the distance r between primary and secondary forces is 2 cm. At low frequency, the equivalent impedance is very similar to the impedance given by a spring, whose stiffness is very large. When the above passive approximation is used instead of the optimal solution, the total power as a function of kr is shown as the dashed line in Fig. 2. As expected, at low values of kr the performance of the passive solution is close to optimum. For values of kr between about 1 and 2, however, the performance of the passive solution is worse than applying no control at all. Appreciable reductions in total power can only be achieved if the secondary force is applied at a distance within $3\lambda_f/8$ from the primary force [14], where λ_f is the frequency-dependent flexural wavelength in the receiving structure. When this distance is 2 cm on a 1.85 mm steel plate, reductions can be achieved up to 550 Hz, while when this distance is 20 cm, the optimal solution is effective only up to 60 Hz.When the value of the stiffness tends to infinity, the system behaves as an infinite plate pinned at the secondary location. In this case, attenuation in the total power for low values of kr is not as great as in the case when $k_a = 1.2 \times 10^6$ N/m. On the other hand, when kr assumes values between 0.5 and 1.5, the pinned case shows better results in terms of total power than the low kr approximation. One way to evaluate the performance of a passive control solution is the ratio of the frequency-averaged power values. This ratio is defined as $P = 10\log_{10}\langle P_c\rangle/\langle P_u\rangle$, where $\langle P_c\rangle$ and $\langle P_u\rangle$ represent, respectively, the power of the controlled

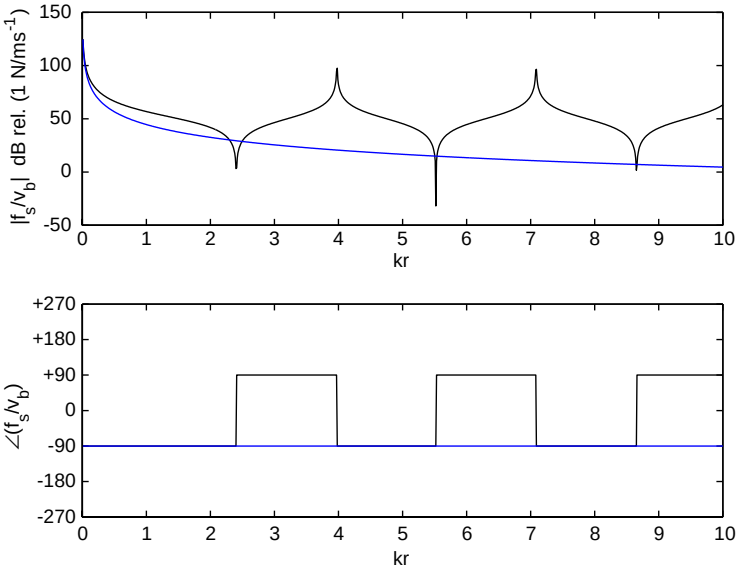

Fig. 3. Equivalent impedance due to the optimal solution (solid black) and comparison with an impedance due to a spring whose stiffness is 1.2×10^6 N/m (faint blue).

and uncontrolled system, averaged over the frequency range 0 Hz–200 Hz. As a function of the passive stiffness constant k_a, the frequency-averaged power ratio reaches a minimum value when $k_a = 2 \times 10^8$ N/m, before it increases slightly and then it settles at the constant value of the averaged power ratio of -0.28 dB, which indicates that the plate is pinned and the system does not benefit from higher values of the stiffness. The choice of $k_a = 1.2 \times 10^6$ N/m is thus appropriate in order to achieve the best possible reduction at low kr, using only a stiffness term, but in order to minimise the averaged power ratio as defined above, it is better to ideally pin the secondary location.

For $kr > 1$, the following Bessel's functions may be replaced with sufficient accuracy by their asymptotic representations [19], and in particular

$$J_0(kr) \cong \sqrt{\frac{2}{\pi kr}} \cos\left(kr - \frac{\pi}{4}\right), \tag{24}$$

$$Y_0(kr) \cong \sqrt{\frac{2\pi}{kr}} \sin\left(kr - \frac{\pi}{4}\right), \tag{25}$$

$$H_0^{(2)}(kr) \cong \sqrt{\frac{2}{\pi kr}} e^{-j(kr-\pi/4)}, \tag{26}$$

Eqs. (1)–(3) describe the terms to be used in Eq. (19) to compute the high-kr approximation of the optimal impedance, which is found to oscillate about

$$Z_{\text{opt}} \cong 8\sqrt{Dm}, \tag{27}$$

which is equal to the infinite plate driving impedance obtained by the reciprocal of equation (1). Fig. 3 shows that, after the stiffness-like behaviour for low values of kr, the optimal solution oscillates about an averaged value given by the driving point impedance of the infinite plate $Z_{00} = 1/Y_{00}$, which is equal to 323 N/m/s for the plate considered above. The equivalent impedance, Eq. (19), is entirely reactive and the mechanism of control, for low kr, is one of the loading primary force, since no power can be absorbed by a reactive impedance. For larger values of kr, the reductions in total power output are far less and the main problem in generating a realisable approximation to the equivalent impedance is the increase in the total power output that occurs at about $kr = 1$ with the equivalent spring, as seen in Fig. 2. It has been found that larger attenuations can be obtained for $kr \cong 1$ if a damper, of value Z_{00}, is connected in parallel with the spring. Fig. 4 shows the total power transmitted to the infinite plate when the secondary force is given by such passive ideal impedance, shown in Fig. 5, and its performance is compared to the optimal case. For values of kr between 3 and 5, the equivalent impedance is either mass or stiffness dominated, whereas this passive approximation to the equivalent impedance is damping dominated, but nevertheless the total power with the equivalent impedance is not very different from the optimal case. Comparing Fig. 2 with Fig. 4, the improved performance due to the new approximation to the equivalent impedance can be noticed. The frequency-averaged power ratio between the controlled system, which uses the spring-damper impedance and the uncontrolled system, as a function of the passive stiffness constant k_a when the damper value is kept constant at 323 N/m/s, shows that the minimum of the curve occurs when $k_a = 1.2 \times 10^6$ N/m. For this configuration of the approximation to the equivalent impedance, the averaged power ratio is about -0.444 dB, and this value is less than the –0.3 dB, which was obtained when implementing a stiffness as an approximation to the equivalent impedance. For large values of the stiffness k_a , the

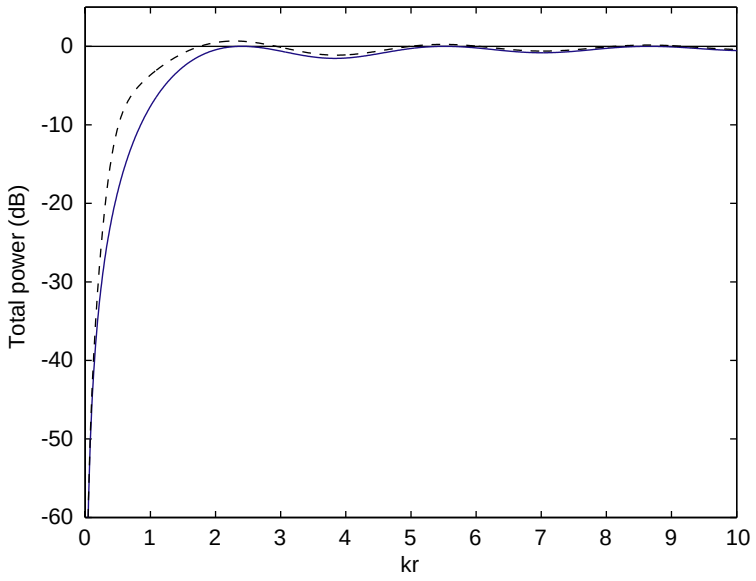

Fig. 4. Total power transmitted to an infinite plate, normalized to that due to the primary force only (solid black), when the primary and optimal secondary forces are applied (faint blue), and when the secondary force is replaced by a spring and a damper, whose stiffness and damping values are $k_a = 1.2 \times 10^6$ N/m and $c_a = 1/Y_{00} = 323$ N/m/s (dashed).

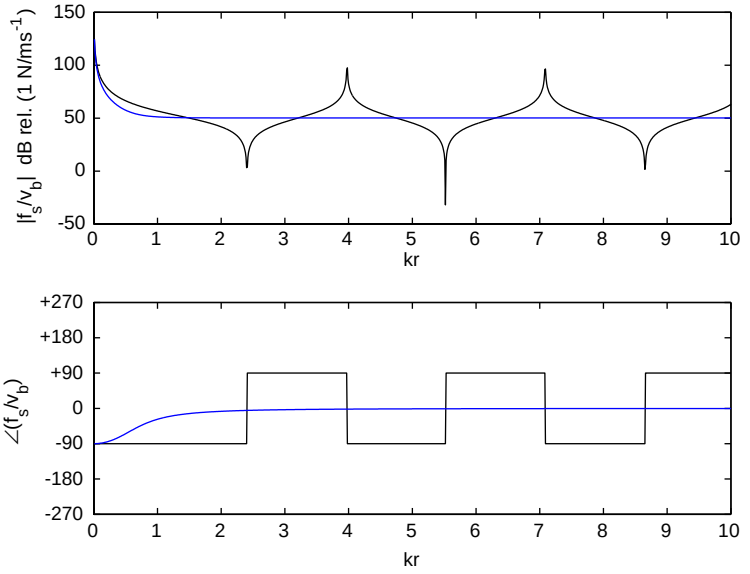

Fig. 5. Equivalent impedance due to the optimal solution (solid black) and comparison with an impedance due to a spring and a damper whose stiffness and damping values are $k_a = 1.2 \times 10^6$ N/m and $c_a = 1/Y_{00} = 323$ N/m/s (faint blue).

ratio tends to –0.28 dB only, showing that for this value, the infinite plate is pinned at the secondary location.

In conclusion, when a secondary force is applied to an infinite plate to counteract the vibrations due to a primary force, the equivalent impedance of the optimal solution to the secondary force can be used to motivate a realisable approximation of the said equivalent impedance, and this is given by the parallel combination of a spring and a damper. The stiffness approximates the behaviour of the optimal solution for small values of kr, while the damping approximates the frequency-averaged behaviour for greater values of kr, as shown in Fig. 5. When the distance between primary and secondary forces is small compared with the flexural wavelength, the important part of the effective passive approximation to the optimal solution is thus the stiffness, while at greater distances, dissipating energy through a damper is the most effective way of controlling the power output. If calculations are performed with a number of primary forces having randomised phases, for which $kr > 1$ in each case, the optimal equivalent impedance to the secondary force, for minimum total power output, also tends to the driving point impedance of an infinite plate, Z_{00}. Since the equivalent impedance can no longer directly load the primary sources, its best strategy is to absorb power, and the impedance which absorbs the maximum power from a network is the conjugate of the network's driving point impedance [6]. This is known as the matched load, and since Z_{00} is real in this case, the matched load is also equal to Z_{00}.

3. Equivalent impedance for global control of vibrating finite plates

In order to apply the optimal solution to a finite plate, we now examine a single-point secondary force f_s acting in P_1 separated by a distance r from a point primary force acting in P_0,

both forces being applied along the z-axis on a finite plate. This configuration is depicted in Fig. 6. In the simulations it is assumed that the $700 \times 500 \times 1.85\,\mathrm{mm}^3$ ($=l_x \times l_y \times h$) plate is clamped on two opposite ends and free to move on the other two. These particular dimensions and boundary conditions were chosen to correspond to those of an experimental plate used in previous investigations [20]. Y_{00} is again the driving point mobility at $P_0 = (x_0, y_0)$, Y_{10} is the transfer mobility when the point of excitation is P_0 and the measurement occurs at $P_1 = (x_1, y_1)$, and Y_{11} is the driving point mobility at P_1. The driving point and transfer mobilities, relating the vertical velocity and the force excitation at the locations P_0 and P_1, can now be derived using a modal superposition approach [21]. The general expression for the mobility Y_{ij} when the force is applied in P_j and the velocity is measured in P_i is given by

$$Y_{ij} = \frac{\mathrm{j}\omega}{M} \sum_{m=1}^{\infty} \sum_{n=1}^{\infty} \frac{\Phi_{mn}(P_i)\Phi_{mn}(P_j)}{\varepsilon_{mn}[\omega_{mn}^2(1+\mathrm{j}\eta) - \omega^2]}, \tag{28}$$

where the indices m and n represent the number of half-standing waves in the x and y directions for the natural mode Φ_{mn}. The term ε_{mn} is a normalising factor [16], M is the total mass of the plate, ω_{mn} is the m,nth natural frequency of the flexural vibration and η is the hysteretic loss factor [16]. The plate under study has two clamped edges and two free edges, therefore an exact solution of the wave equation and the boundary condition equations cannot be found. Thus an approximate solution must be used [22]. The expressions for the terms in Eq. (28) can be found in Refs. [22,23].

The cost function given by the sum of the power input due to the primary and secondary force, $\Pi = \Pi_p + \Pi_s$, can still be expressed in the quadratic form of Eq. (5)–(8) and thus be minimised with an optimum secondary force. The total power due to the primary force only, Eq. (9), is compared in Fig. 7 with the total power described in Eq. (10) when the secondary force is given by the optimal solution described by Eq. (11). Fig. 7 shows the power supplied to the finite plate due to the primary force only (solid line), applied at an arbitrary location $P_0 = (0.32\,\mathrm{m}, 0.27\,\mathrm{m})$, and due to the combination of the primary and optimal secondary force (faint line), applied at a distance $r = 2\,\mathrm{cm}$, at the location $P_1 = (0.3059\,\mathrm{m}, 0.2841\,\mathrm{m})$ from the primary. The reduction is substantial, with some of the modes being almost cancelled, while others are greatly reduced. This is due to the particular location that was chosen for the secondary force. At that location, the secondary force can couple into most modes, but this location is either on or close to the nodal

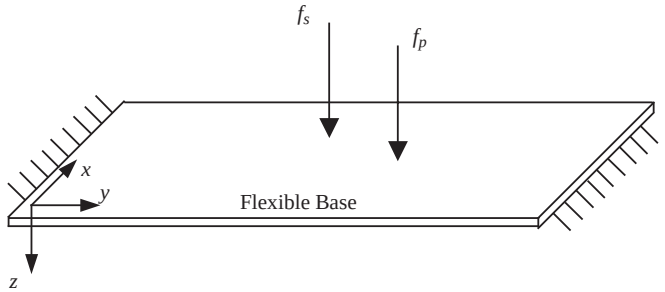

Fig. 6. A point primary force and a point secondary force applied to a finite $700 \times 500 \times 1.85\,\mathrm{mm}^3$ plate clamped on two opposite edges and free on the other two edges.

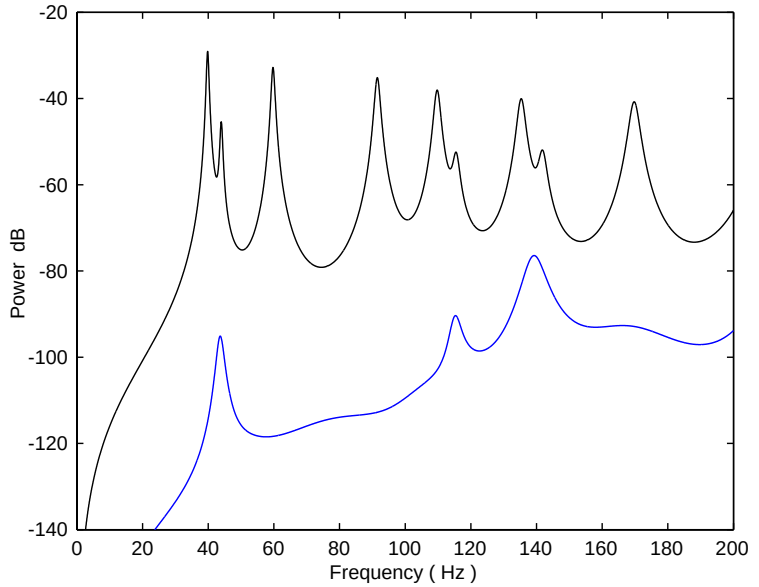

Fig. 7. Total power transmitted to the finite plate due to the primary force only (solid black) and due to the primary and secondary forces when the optimal feedforward solution is applied and the distance between primary and secondary force is 2 cm (faint blue).

lines of those modes that are not completely flattened out. The impedance that the secondary force has to present to the system in order to minimise the total power is obtained by computing the optimal secondary force per unit velocity at the secondary location, f_{so}/v_{so}. The velocity of the base v_{so} at P_1 when the optimal solution is implemented is given by

$$v_{so} = Y_{10} f_p + Y_{11} f_{so}. \tag{29}$$

Substituting Eq. (11) into Eq. (29), the equation becomes

$$v_{so} = Y_{10} f_p - Y_{11} \left(\frac{\mathrm{Re}(Y_{10})}{\mathrm{Re}(Y_{11})} \right) f_p, \tag{30}$$

which represents the velocity as a function of the primary force. Combining equations (11) and (30), the equivalent impedance when the optimal secondary force is implemented can be obtained. It is given by

$$Z_{opt} = \frac{f_{so}}{v_{so}} = \frac{\mathrm{Re}(Y_{10})}{\mathrm{Re}(Y_{10}) Y_{11} - \mathrm{Re}(Y_{11}) Y_{10}}. \tag{31}$$

This equivalent impedance, which is again entirely reactive, is shown in Fig. 8, where it can be seen that sharp transactions occur between the stiffness and the mass-dominated regions. Between 0 and about 45 Hz, the impedance is stiffness dominated, as it is between about 60 and 120 Hz, and between 155 and 175 Hz. In the remaining intervals within the 0~200 Hz window, the impedance is mass dominated. As for the infinite plate case, this impedance is non-causal [18] as it can be

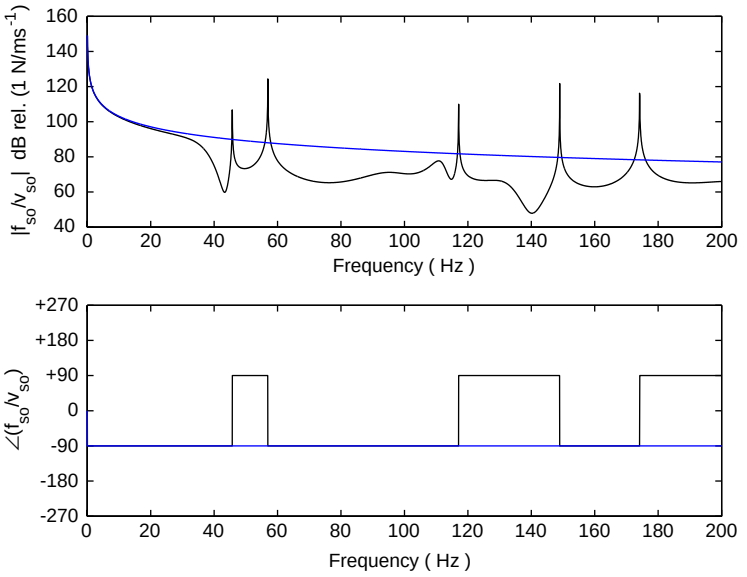

Fig. 8. Equivalent impedance due to the optimal secondary force (solid black) and the impedance of an ideal stiffness whose value is $k_a = 9 \times 10^6$ N/m (faint blue). The distance between primary and secondary force is 2 cm and the plate is finite. It can be noted that the real part of the impedance is zero.

verified by computing the FFT of the result shown in Fig 8. Eq. (31) can be rewritten as

$$Z_{\text{opt}} = \frac{1}{Y_{11} - \frac{\text{Re}(Y_{11})}{\text{Re}(Y_{10})} Y_{10}}, \tag{32}$$

where, from Eq. (28),

$$\text{Re}(Y_{11}) = \sum_{m=1}^{\infty} \sum_{n=1}^{\infty} \frac{\Phi_{mn}^2(P_1) \omega \omega_{mn}^2 \eta}{\Lambda_{mn}[(\omega_{mn}^2 - \omega^2)^2 + \eta \omega_{mn}^4]} \tag{33}$$

and

$$\text{Re}(Y_{10}) = \sum_{m=1}^{\infty} \sum_{n=1}^{\infty} \frac{\Phi_{mn}(P_1) \Phi_{mn}(P_0) \omega \omega_{mn}^2 \eta}{\Lambda_{mn}[(\omega_{mn}^2 - \omega^2)^2 + \eta \omega_{mn}^4]}. \tag{34}$$

At very low frequency the ratio between the real parts in Eq. (32) can be approximated by taking only the first modal term, in which case

$$\frac{\text{Re}(Y_{11})}{\text{Re}(Y_{10})} \cong \frac{\Phi_{11}(P_1)}{\Phi_{11}(P_0)}. \tag{35}$$

The mode shape of the first mode can be found in Ref. [23], and at low frequency, for the chosen locations, from Eq. (35), then $\text{Re}(Y_{11})/\text{Re}(Y_{10}) \cong 0.84$. At very low frequencies the driving point

mobility Y_{11} can also be approximated by

$$Y_{11} \cong \mathrm{j}\omega \frac{\Phi_{mn}^2(P_1)}{M\varepsilon_{mn}\omega_{mn}^2}, \tag{36}$$

where

$$\omega_{11} = \sqrt{\frac{Eh^2}{12\rho(1-\upsilon^2)}}\left(\frac{\pi}{l_x}\right)^2 q_{22}. \tag{37}$$

The expression for the coefficient q_{22} is provided in Ref. [23] and the normalising factor ε_{11} can be approximated using the factor for the free-free boundary condition, which is given by $\varepsilon_{11} \cong \frac{1}{4}$. Substituting the appropriate values in the above equations, a low-frequency approximation to the equivalent impedance Z_{opt} in equation (32) is given by

$$\begin{aligned} Z_{\mathrm{opt}} &\cong \frac{\pi^4 Eh^3 l_y q_{22}^2}{\mathrm{j}\omega 48(1-\upsilon^2) l_x^3 \Phi_{11}(P_1)[\Phi_{11}(P_1) - 0.84\Phi_{11}(P_0)]} \\ &\cong \frac{9\times 10^6}{\mathrm{j}\omega}. \end{aligned} \tag{38}$$

As well as the equivalent impedance in the optimal case, Fig. 8 also shows the low-frequency approximation to the impedance given by a spring, whose stiffness is $k_a = 9\times 10^6$ N/m.

When the distance r is equal to 20 cm, not as much attenuation in the total power is obtained, as shown in Fig. 9. The optimal impedance also has lower average values, compared to the case when $r = 2$, as shown in Fig. 10, which also shows the impedance of a spring, whose stiffness is $k_a = 2.5\times 10^5$ N/m, that has been computed in an analogous way to that above.

When the relative distance between primary and secondary forces is large and at low frequency, the driving point mobility dominates the transfer mobility in Eq. (32). Hence, when $|Y_{11}| \gg |Y_{10}|$ then $Z_{\mathrm{opt}} \cong Z_{11} = 1/Y_{11}$. Eq. (36) provides the approximation of the expression for the driving point mobility at low frequency and it is equivalent to a stiffness of about 7×10^4 N/m. In the simulations, this is the value of the stiffness that approximates the low-frequency behaviour when the relative distance $r = 80$ cm.

At high frequency or large relative distances r, the characteristic driving point or transfer mobility are equal to the driving point or transfer mobility of an infinite plate [19]. Consequently, Eqs. (12) and (13) describe the real part of the driving point and transfer mobility for an infinite plate, while Eqs. (1)–(3) describe the remaining terms to be used in Eq. (32) to compute the high-kr approximation to the equivalent impedance, which is found to oscillate about a value which is equal to the infinite plate driving impedance. Assuming a constant location of the secondary force, and varying the location of the primary force on the plate, it is found that for small relative distances between the primary and secondary forces, the average of the optimal equivalent impedance above 40 Hz can be approximated using a larger damper, whose maximum damping value was found to be about $c_a = 4000$ N/m/s when the distance $r = 2$ cm. For large distances between primary and secondary forces, the averaged equivalent impedance can be approximated using lower values of the damping. The minimum value that was found is about $c_a = 323$ N/m/s when the distance $r = 80$ cm, as expected from the above discussion. This indicates that even for

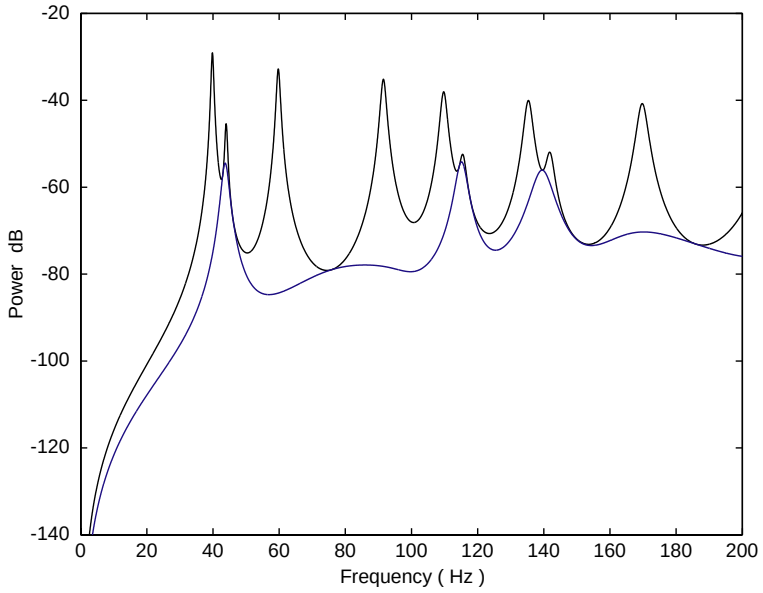

Fig. 9. Total power transmitted to the finite plate due to the primary force only (solid black) and due to the primary and secondary forces when the optimal feedforward solution is applied and the distance between primary and secondary force is 20 cm (faint blue).

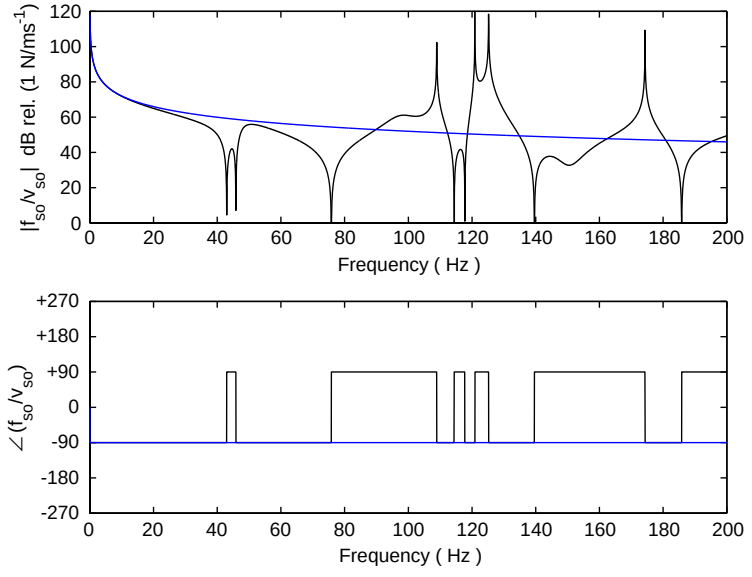

Fig. 10. Equivalent impedance due to the optimal secondary force (solid black) and the ideal stiffness whose value is $k_a = 2.5 \times 10^5$ N/m. The distance between primary and secondary force is 20 cm and the plate is finite. It can be noted that the real part of the impedance is zero.

finite plates, a simplified approximation to the equivalent impedance is given by the parallel of a spring and a damper.

4. Optimising the spring/damper approximation to the equivalent impedance

The primary drawback of the optimal equivalent impedance shown in Figs. 8 and 10 is that it is non-causal and so cannot be implemented with broadband random excitations. Therefore, other solutions have been investigated even though their performance will be worse than that one provided by the optimal solution. In this section, the combination of an optimum stiffness and a damper will be analysed. Firstly, the two solutions are investigated independently, then they will be considered together, acting in parallel on the finite plate. The relative distance, r, between primary and secondary forces is assumed to be 2 cm for these simulations.

4.1. Control with a spring

Fig. 11 shows the ratio of the frequency-averaged power, P , as defined above, as a function of stiffness. The function descends monotonically until it flattens off at about $k_a = 9 \times 10^6$ N/m, which indicates the minimum value of stiffness that provides the greatest attenuation in power (about 14 dB). At low values of the stiffness, the ratio of the frequency averaged power is very steep. Fig. 12 shows the total power when the stiffness is chosen to be $k_a = 9 \times 10^6$ N/m (dashed

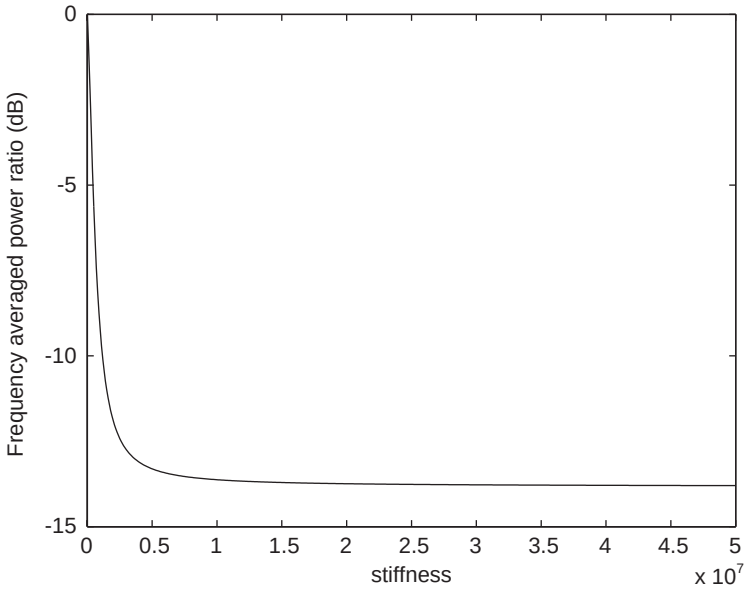

Fig. 11. Ratio of the uncontrolled to controlled frequency-averaged power, as a function of the stiffness value k_a. After about $k_a = 9 \times 10^6$ N/m, the average power ratio does not improve much. The distance between primary and secondary forces is 2 cm.

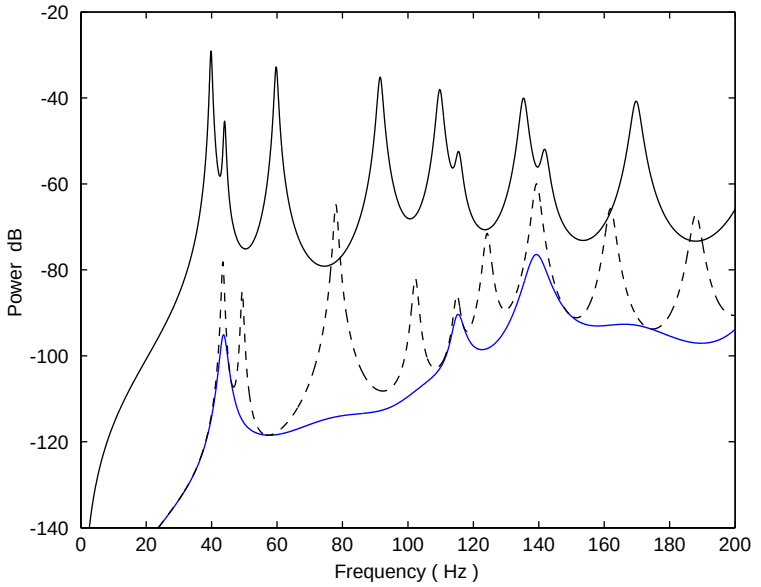

Fig. 12. Total power transmitted to the finite plate due to the primary force only (solid black), the primary and secondary forces when the optimal feedforward solution (faint blue), and the primary and secondary forces when the ideal displacement feedback is implemented and the stiffness is $k_a = 9 \times 10^6$ N/m (dashed). The distance between primary and secondary force is 2 cm.

line), compared to the optimal solution (faint line) and the uncontrolled case (solid line). It can be noted that high attenuations can be achieved at low frequency due to the similarity between optimal solution and passive equivalent approximation. Although $k_a = 9 \times 10^6$ N/m seems to be a good choice at low frequency, as discussed above, at higher frequency its effect is merely to pin the structure at the secondary location and therefore a redistribution of the resonances is experienced.

4.2. Control with a damper

Fig. 13 shows the ratio of the frequency-averaged power, P, as a function of damping c_a introduced at P_1. The minimum of the function at about $c_a = 4000$ N/m/s is -14.5 dB, and it indicates the value of damping that provides the greater attenuation in terms of power. At low gains, the frequency-averaged power is very steep then, after reaching a minimum value, it settles towards the constant value –14 dB, which indicates that the system is pinned and it does not benefit from higher damping values. This limiting value is the same as that in Fig. 11. Fig. 14 shows the total power when $c_a = 4000$ N/m (dashed line), compared to the optimal solution (faint line) and the uncontrolled case (solid line). Compared to Fig. 12, lower attenuations are experienced below the first plate resonance and higher attenuations can be achieved at high frequency.

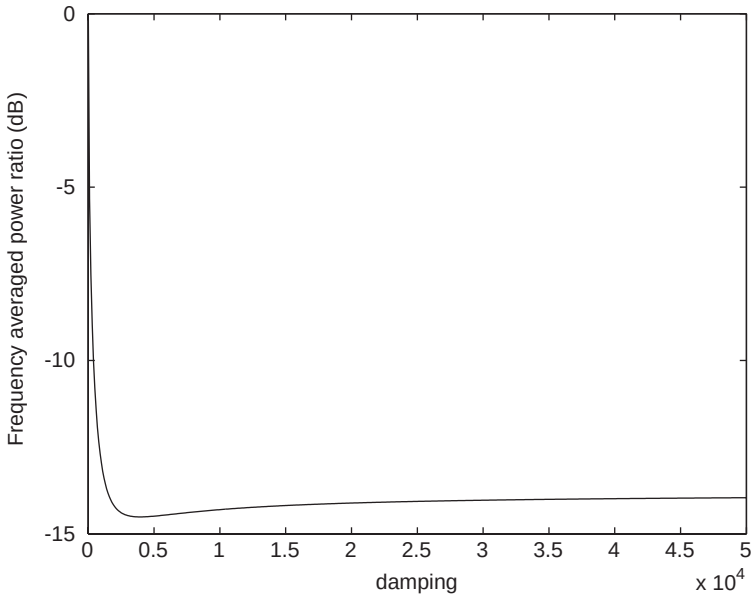

Fig. 13. Ratio of the uncontrolled to controlled frequency-averaged power, as a function of the damping value c_a. The minimum of the function at about $c_a = 4000\,\mathrm{N/m/s}$ indicates the value of the gain that provides the greater attenuation in terms of power. The distance between primary and secondary forces is 2 cm.

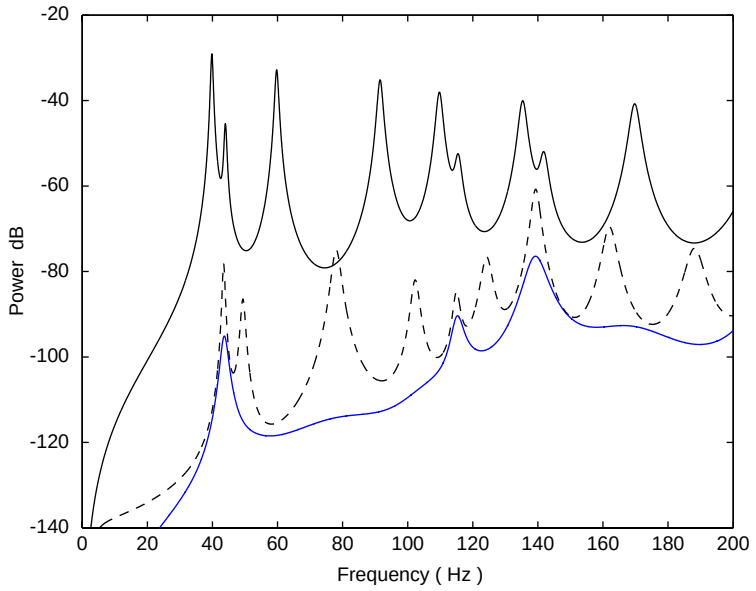

Fig. 14. Total power transmitted to the finite plate due to the primary force only (solid black), the primary and secondary forces when the optimal feedforward solution is applied (faint blue), and the primary and secondary forces when the ideal velocity feedback is applied and the damping value $c_a = 4000\,\mathrm{N/m/s}$ (dashed). The distance between primary and secondary force is 2 cm.

4.3. Control with a spring and a damper

We now assume that the secondary force is generated by a spring and a damper, whose values are chosen by a joint optimisation. Fig. 15 shows the contour plot of the ratio of the frequency-averaged power, P, as a function of damping and stiffness. The ratio is maximum at the origin, then it descends. The minimum of the function (about –14.62 dB) occurs when the damping value $c_a = 4{,}000\,\mathrm{N/m/s}$, which coincides with the minimum of the curve in Fig. 13, and the stiffness value $k_a = 5.5 \times 10^5\,\mathrm{N/m}$. Fig. 16 shows both the equivalent impedance of the optimal solution and the impedance of the chosen spring–damper system. In particular, the passive approximation does not match the equivalent impedance at low frequency, and this is due to the particular choice made for the stiffness, which minimises the frequency averaged power. Fig. 17 shows the total power when the chosen spring–damper system is applied (dashed line). Compared to Fig. 14, the system clearly benefits at low frequency from the stiffness, and above the first plate resonance, it benefits from the energy that has been taken away by the damper. Compared to Figs. 12 and Fig. 14, this case provides a better performance.

In summary, although the power reduction due to the parallel of a stiffness term and a damping term is greater than the results obtained by using either a spring or a damper, the difference in frequency-averaged power between the parallel case and the single cases is not substantial. This result holds for the case where the relative distance between primary and secondary forces is relatively small and the frequency band of interest includes low- and high-frequency components. These conditions are often met in practical vibration isolation problems, while for limit cases, at

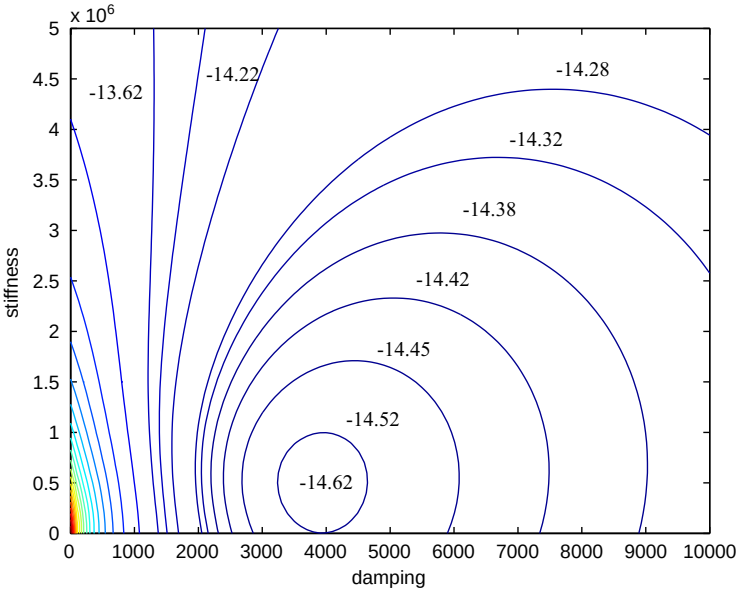

Fig. 15. Contour plot of the ratio of the uncontrolled to controlled frequency-averaged power, as a function of the damping value c_a and the stiffness value k_a. The minimum of the function at –14.62 dB occurs when $c_a = 4000\,\mathrm{N/m/s}$ and $k_a = 5.5 \times 10^5\,\mathrm{N/m}$. The distance between primary and secondary forces is 2 cm.

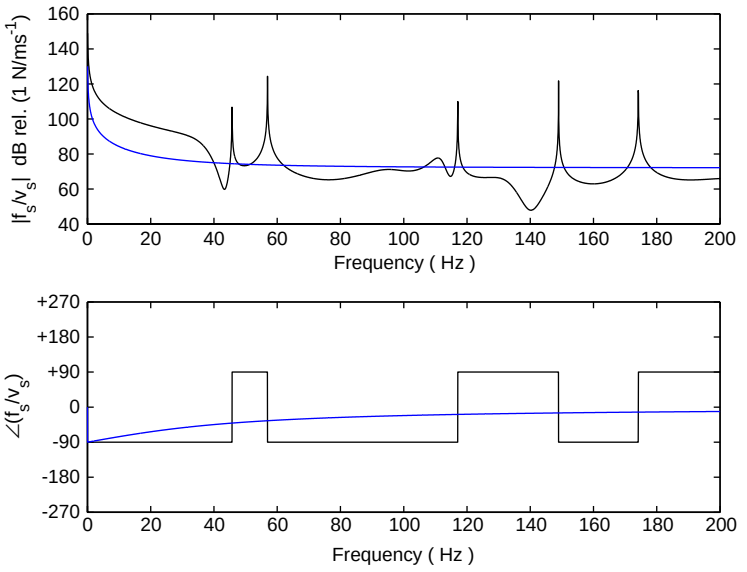

Fig. 16. Equivalent impedance due to the optimal secondary force (solid black) and the ideal displacement and velocity feedback control, where the stiffness value $k_a = 5.5 \times 10^5$ N/m and the damping value $c_a = 4000$ N/m/s (dashed). The distance between primary and secondary force is 2 cm.

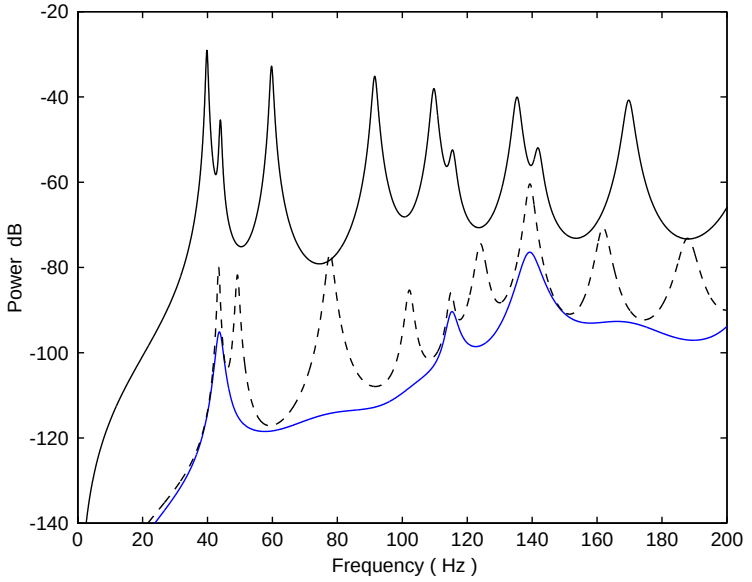

Fig. 17. Total power transmitted to the finite plate due to the primary force only (solid black), the primary and secondary forces when the optimal feedforward solution is applied (faint blue), and the primary and secondary forces when the ideal displacement and velocity feedback is applied, where the stiffness value $k_a = 5.5 \times 10^5$ N/m and the damping value $c_a = 4000$ N/m/s (dashed). The distance between primary and secondary force is 2 cm.

very low or very high frequency, or very short or very long relative distances, as discussed above, the equations derived previously are valid.

5. Conclusions

In this study the total power of the forces exerted on a structure was chosen to be the cost function to be minimised. In particular, the effect of the distance between primary and secondary excitations was taken into account and simulations were run for both infinite and finite plates.

The core of this study was the comparison between optimal solutions and the performance of idealised passive control treatments. In particular, the optimised equivalent impedance for global control was compared to its passive approximation. It was found that, although the equivalent impedance is able to provide a substantial total power reduction compared to the other treatments, ideal passive solutions, based on the parallel configuration of a spring and a damper, can guarantee a good power reduction. The locations of the primary and secondary excitations and their relative distance may become an important aspect of the design of the panel vibration controller. In fact, depending on the location of the primary force with respect to the nodal lines, the power distribution of the uncontrolled system changes and, depending on the location of the secondary force with respect to the nodal lines, the optimal solution turns out to be more or less effective. Unfortunately, in many practical applications a rigid ground is not available and therefore these idealised passive solutions cannot be implemented. The development of devices using inertial actuators [10] that can be industrially manufactured in order to provide substantial attenuation in panel vibration is under study.

References

[1] M.J. Brennan, J. Dayou, Global control of vibration using a tunable vibration neutralizer, *Journal of Sound and Vibration* 232 (3) (2000) 585–600.
[2] O. Bardou, P. Gardonio, S.J. Elliott, R.J. Pinnington, Active power minimization and power absorption in a plate with force and moment excitation, *Journal of Sound and Vibration* 208 (1) (1997) 111–151.
[3] M.J. Brennan, S.J. Elliott, R.J. Pinnington, Strategies for the active control of flexural vibration on a beam, *Journal of Sound and Vibration* 186 (4) (1995) 657–688.
[4] M.J. Brennan, Control of flexural waves on a beam using a tunable vibration neutraliser, *Journal of Sound and Vibration* 222 (3) (1998) 389–407.
[5] C.Q. Howard, S.D. Snyder, C.H. Hansen, Calculation of vibratory power transmission for use in active vibration Control, *Journal of Sound and Vibration* 233 (4) (2000) 573–585.
[6] S.J. Elliott, P. Joseph, P.A. Nelson, M.E. Johnson, Power output minimizations and power absorption in the active control of sound, *Journal of Acoustic Society of America* 90 (5) (1991) 2501–2512.
[7] N. Tanaka, Y. Kikushima, Rigid support active vibration isolation, *Journal of Sound and Vibration* 125 (3) (1988) 539–553.
[8] S.J. Elliott, The control of transmitted power in an active isolation system, *Proceedings of the ACTIVE 97*, Budapest, Hungary, August 21–23 1997.
[9] P.A. Nelson, S.J. Elliott, *Active Control of Sound*, Academic Press, New York, 1992.
[10] L. Benassi, S.J. Elliott, Global control of a vibrating plate using a feedback-controlled inertial actuator, *Journal of Sound and Vibration* 283 (1 + 2) (2005) 69–90, this issue; doi:10.1016/j.jsv.2004.03.039.

[11] P.J. Titterton, Synthesis of optimal, single-frequency, passive control laws, with applications to reducing the acoustic radiation from a submerged spherical shell, *Journal of the Acoustical Society of America* 105 (4) (1999) 2261–2268.
[12] D. Guicking, J. Melcher, R. Wimmel, Active impedance control II: mechanical structures, *Acoustica* 69 (1989) 39–52.
[13] J. Yuan, Global damping of noise or vibration fields with locally synthesized controllers, *Journal of the Acoustical Society of America* 111 (4) (2002) 1726–1733.
[14] C.R. Fuller, S.J. Elliott, P.A. Nelson, *Active Control of Vibration*, Academic Press, New York, 1997.
[15] M.D. Jenkins, P.A. Nelson, R.J. Pinnington, S.J. Elliott, Active isolation of periodic machinery vibrations, *Journal of Sound and Vibration* 166 (1) (1993) 117–140.
[16] L. Cremer, M. Heckl, E.E. Ungar, *Structure-borne Sound*, Springer, Berlin, 1988.
[17] M. Abramowitz, I.A. Stegun, *Handbook of Mathematical Functions*, Dover, New York, 1972.
[18] D.W. Miller, S.R. Hall, A.H. von Flotow, Optimal control of power flow at structural junctions, *Journal of Sound and Vibration* 140 (3) (1990) 475–497.
[19] E. Skudrzyk, *Simple and Complex Vibratory Systems*, The Pennsylvania State University Press, Pittsburgh, 1968.
[20] L. Benassi, S.J. Elliott, P. Gardonio, Active vibration isolation using an inertial actuator with local force feedback control, *Journal of Sound and Vibration* 276 (1–2) (2004) 157–179.
[21] W. Soedel, *Vibration of Shells and Plates*, Marcel Dekker, New York, 1993.
[22] A.W. Leissa, *Vibration of Plates*, NASA SP-160, 1969.
[23] R.E.D. Bishop, D.C. Johnson, *The Mechanics of Vibration*, Cambridge University Press, Cambridge, MA, 1960.